Centralized Control System Design for Underwater Transportation using two Hovering Autonomous Underwater Vehicles (HAUVs)

Rehman, F.U.*, Thomas, G., Anderlini, E.*****

*University College London, UK
e-mail: ucemfre@ ucl.ac.uk

** University College London, UK
e-mail: giles.thomas@ ucl.ac.uk

*** University College London, UK
e-mail: e.anderlini@ ucl.ac.uk

Abstract: In this paper, a centralized control system is designed for the two HAUVs undertaking underwater transportation of a spherical payload via cylindrical manipulators. First, the nonlinear coupled dynamic model is developed considering the rigid body connection method for transportation. The effect of the hydrodynamic, hydrostatic and thrust parameters are taken about the centre of the combined body i.e. the centre of payload. Path trajectory is generated using the minimum snap trajectory algorithm. The trajectory is divided into segments for each directional motion which is further divided into the waypoints based on the time step of the duration. The path between two waypoints is represented by a 7th order polynomial. The centralized control system is designed to follow the desired trajectory. The control system is designed using PID controllers for the motion control in each direction. The main technical requirements are the stability of the payload, accurate trajectory tracking and robustness to overcome uncertainties. Stability cannot be compromised because of the rigid connection between the vehicles and the payload, whereas, tracking is given a tolerance of ±5%. Transportation task is observed for the desired motion in the horizontal plane. The time domain motion simulation results show that the desired trajectory has been accurately followed by the combined system while meeting the technical requirements.

Keywords: Rigid body connection, Nonlinear coupled dynamic model, hydrodynamics, path trajectory, waypoints, PID controller, tracking.

1. INTRODUCTION

Unmanned Underwater Vehicles (UUVs) have been increasingly used in underwater operations [1]. They can be used in conditions and can perform tasks which are difficult for humans [2]. Moreover, this can help to reduce risk on human life in dangerous operations [3]. However, these vehicles are small and have less capacity, and therefore, are not feasible to be used stand alone. Hence, multiple UUVs are considered which can provide advantages such as transporting larger loads, flexibility in the number of vehicles used and fault tolerance [4].

The two main types of UUVs are Remotely Operated Vehicle (ROV) and Autonomous Underwater Vehicle (AUV). ROV is mainly considered a tethered vehicle which is connected via umbilical cable for transferring power and communication [5]. AUV, on the other hand, is an untethered vehicle which contains its own power and controls itself while accomplishing a pre-defined task [6]. Conventional AUVs are stable at high speed. However, in recent years, AUVs have been developed for the slow operations which are called hovering AUVs (HAUVs) [7]. Moreover, ROVs can also be modified to operate autonomously. In this work, Minerva ROVs are modified to operate as HAUVs for payload transportation.

Underwater transportation using multiple UUVs can be beneficial in many applications. For instance, it is vital in military applications such as the transportation of emergency damage repair kit to reach the damaged submarine in deep waters or the transportation of equipment for the destruction of identified mines. Moreover, it can be used for short range transportation of a damaged submarine to safe waters. The other important field where underwater transportation could be useful is the oil and gas industry [8]. The extraction rigs which are required to be installed on the seabed could be transported underwater and installed in position with precision. Moreover, during the construction of offshore platforms, the underwater structural members could be transported using multiple underwater vehicles and installed in position.

Widespread research has been conducted on transportation using multiple land and aerial vehicles. The three methods are deduced i.e. rigid body connection, flexible connection and formation keeping using formation control strategy. In the rigid body connection, the vehicles and the payload are rigidly connected through manipulators. For mathematical modelling, a dynamic model is developed for the entire system considering it a single rigid body [9]. In the flexible connection method, a configuration is established for the vehicles such that the payload is in static equilibrium at the desired position

and orientation (pose) keeping in consideration the constraints on cable tension and the payload stability [10]. In the formation keeping approach, the vehicles maintain a formation relative to the payload while transporting it towards the target location. The formation is maintained by means of communication between the vehicles and the payload [11].

The underwater environment is complex compared to land and air, making the implementation of the above mentioned multi-vehicular transportation methods quite challenging. For the land vehicles, the only significant term considered in analysing the motion response is friction, while for the aerial vehicles, gravity is considered the only dominant term [10]. The aerodynamic terms which could have made the analysis quite challenging are ignored due to their less significant values resulting from the small values of density and viscosity of air. On the other hand, underwater vehicles experience some substantial parameters such as the hydrodynamic parameters which consist of the added mass and the damping terms, and the hydrostatic parameters which are influenced by the significant buoyancy effect. Moreover, underwater dynamics is highly nonlinear and coupled.

2. NONLINEAR COUPLED DYNAMIC MODEL

For the design of a control system, the dynamic model is first developed. Dynamic model is a mathematical representation of the actual system which is represented by the equations of motion and includes the rigid body kinematics and kinetics. This saves the cost of experiments as well as time to evaluate different conditions and situations.

The dynamic model can be developed either nonlinear or linear. In this paper, a nonlinear coupled dynamic model is preferred due to its accurate representation of the actual system. However, this requires calculation of several parameters as well as complicates the development of dynamic model compared to the linear model. Moreover, higher control gains are required of the controllers in the control system design to get the desired motion response while following a trajectory. The dynamic model is developed following the approach used by Thor I. Fossen [12].

2.1 Reference frames

The reference frames are first defined i.e. body-fixed and earth-fixed as shown in Figure 1. The velocity and force terms are represented in the body-fixed frame, whereas, positions and orientations are represented in the earth-fixed frame. To get full advantage of the geometric aspects of the body, all the parameters are transformed about the centre of body (O).

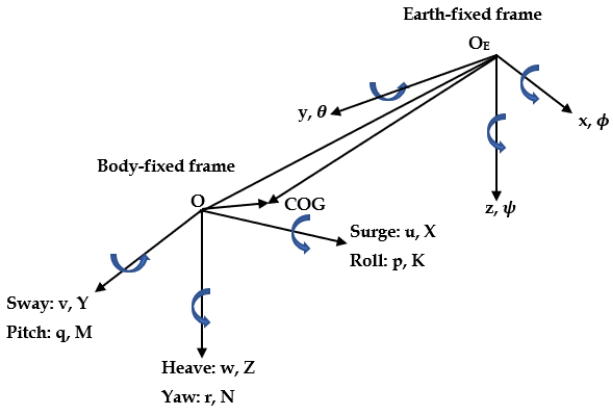

Figure 1: Reference frames [13]

The positions in surge, sway and heave are represented by x, y and z, whereas, orientations in roll, pitch and yaw are denoted by ϕ, θ and ψ respectively. Moreover u, v and w are the translational velocities in surge, sway and heave, whereas, p, q and r are the angular velocities in roll, pitch and yaw respectively. Similarly, X, Y and Z are the forces in surge, sway and heave, whereas, K, M and N are the moments in roll, pitch and yaw respectively. Right hand rule is applied such that surge is positive forward, sway is positive right, and heave is positive down.

2.2 Assumptions

The assumptions taken in the development of dynamic model are 1) vehicle is a rigid body i.e. the distance between any mass particle on the body and the centre of body does not change by the application of forces [14]. Therefore, there is no force variation between the mass particles 2) mass and its distribution do not change during the operation of the vehicle. 3) vehicle is deeply submerged so the wave effects are ignored. 4) interaction effects with other bodies are ignored. 5) Sea currents are ignored. Moreover, assumptions are made while calculating the hydrodynamic parameters using the empirical data. For instance, DNV standards are used which assumes that the vehicle has 3 planes of symmetry and two of the three sides are equal in dimension or the difference is up to 10% [15]. These assumptions bring about uncertainties in the dynamic model which require the design of a robust control system.

2.3 Development of dynamic model

Due to the use of same Minerva HAUVs and manipulators, which are attached to the spherical payload in the centre, the combined system has three planes of symmetry. The product of inertia and hydrostatic moment terms are zero. Moreover, only the diagonal hydrodynamic parameters are considered. The nonlinear coupled equations of motion in 6 DOF of the combined system is shown as [12]

$$
\begin{aligned}
&(m - X_{\dot{u}})\dot{u} + m(wq - vr) - Z_{\dot{w}}wq + Y_{\dot{v}}vr - X_u u \\
&- X_{u|u|}u|u| + (W - B)sin\theta = \tau_X,
\end{aligned}
$$

$$
\begin{aligned}
&(m - Y_{\dot{v}})\dot{v} + m(ur - wp) + Z_{\dot{w}}wp - X_{\dot{u}}ur - Y_v v \\
&- Y_{v|v|}v|v| - (W - B)cos\theta sin\phi = \tau_Y,
\end{aligned}
$$

$$
\begin{aligned}
&(m - Z_{\dot{w}})\dot{w} + m(vp - uq) - Y_{\dot{v}}vp + X_{\dot{u}}uq - Z_w w \\
&- Z_{w|w|}w|w| - (W - B)cos\theta cos\phi = \tau_Z,
\end{aligned}
$$

$$
\begin{aligned}
&(I_x - K_{\dot{p}})\dot{p} + (I_z - I_y)qr + (Y_{\dot{v}} - Z_{\dot{w}})vw + (M_{\dot{q}} - N_{\dot{r}})qr \\
&- K_p p - K_{p|p|}p|p| - z_b B cos\theta sin\phi = \tau_K,
\end{aligned}
$$

$$
\begin{aligned}
&(I_y - M_{\dot{q}})\dot{q} + (I_x - I_z)rp + (Z_{\dot{w}} - X_{\dot{u}})uw \\
&+ (N_{\dot{r}} - K_{\dot{p}})pr - M_q q - M_{q|q|}q|q| - z_b B sin\theta = \tau_M,
\end{aligned}
$$

$$
\begin{aligned}
&(I_z - N_{\dot{r}})\dot{r} + (I_y - I_x)pq + (X_{\dot{u}} - Y_{\dot{v}})uv + (K_{\dot{p}} - \\
&M_{\dot{q}})pq - N_r r - N_{r|r|}r|r| = \tau_N.
\end{aligned}
\qquad (1.\ 1)
$$

Where m is the mass of the combined system which includes the masses of the HAUVs, manipulators and payload. W and B are the weight and buoyancy, I_x, I_y, I_z are the moment of inertia terms, $X_{\dot{u}}$, $Y_{\dot{v}}$ and $Z_{\dot{w}}$ are the translational added mass terms, while, $K_{\dot{p}}$ $M_{\dot{q}}$ and $N_{\dot{r}}$ are the rotational added mass terms, X_u, Y_v, Z_w, K_p, M_q and N_r are the linear damping terms, whereas, $X_{u|u|}$, $Y_{v|v|}$, $Z_{w|w|}, K_{p|p|}$, $M_{q|q|}$ and $N_{r|r|}$ are the quadratic damping terms and finally, $\tau_X, \tau_Y, \tau_Z, \tau_K, \tau_M$ and τ_N are the actuator forces and moments for the combined system respectively.

The moment of inertia terms and hydrodynamic parameters for the cylindrical manipulators and the spherical payload are calculated using the derived equations and empirical data respectively [15]–[20], whereas, these are taken from reference [21] for the Minerva HAUV. The hydrostatic parameters are selected such that the manipulators and HAUVs are neutrally buoyant while the weight of the payload is selected in such a manner that the difference between weight and buoyancy is within the range of the vertical thrusters on the two HAUVs.

For the generation of the algorithm for simulation, equation (1. 1) is used in matrix form, which is given as [12]

$$\boldsymbol{M\dot{v} + C(v)v + D(v)v + g(\eta) = \tau}. \qquad (1.\ 2)$$

Where

$\boldsymbol{M = M_{RB} + M_A} -$

Mass Matrix $=$ Rigid body $+$ Added mass matrices

$\boldsymbol{C(v) = C_{RB}(v) + C_A(v)} -$

Coriolis matrix $=$ Rigid body + Added mass Coriolis matrices

$\boldsymbol{D(v) = D_L(v) + D_Q(v)}$

Damping matrix $=$ Linear $+$ Quadratic damping matrices

$\boldsymbol{g(\eta)} -$ Vector of hydrostatic forces and moments

$\boldsymbol{\tau} -$ Actuators′ thrust vector

3. PROPULSION MODEL

To develop the propulsion model for the combined system of two HAUVs, the thrust vector of each thruster must be worked out which is given as [22]

$$\boldsymbol{\tau_{t_i}} = \begin{bmatrix} \boldsymbol{f} \\ \boldsymbol{l_{t_i}} \times \boldsymbol{f} \end{bmatrix} = \begin{bmatrix} f_x \\ f_y \\ f_z \\ l_y f_z - l_z f_y \\ l_z f_x - l_x f_z \\ l_x f_y - l_y f_x \end{bmatrix}. \qquad (1.\ 3)$$

$\boldsymbol{f}$ is the thrust force vector of the thruster and $\boldsymbol{l_{t_i}}$ is the distance of that thruster from the combined centre of body (O).

The system under study consists of 10 thrusters (5 on each HAUV). Therefore, it is recommended to write the thrust vector as a product of thrust allocation matrix ($\boldsymbol{T_a}$) and thrust force vector ($\boldsymbol{f}$)

$$\boldsymbol{\tau = T_a f}. \qquad (1.\ 4)$$

The thrust force vector of the combined system is written as

$$\boldsymbol{f} = [f_1\ f_2\ f_3\ f_4\ f_5\ f_6\ f_7\ f_8\ f_9\ f_{10}]^{\boldsymbol{T}}. \qquad (1.\ 5)$$

f_1 and f_6 are the thrust forces of the transverse thrusters, f_2, f_3 and f_7, f_8 are the thrust forces of the vertical thrusters and f_4, f_5 and f_9, f_{10} are the thrust forces of the axial thrusters respectively.

The contribution of each thruster in the combined system is required to be allocated in the propulsion model. This helps to get the effect of each thruster about the combined centre of body (O). The columns in the thrust allocation matrix ($\boldsymbol{T_a}$) represent the contribution of each thruster installed on the combined system. It depends on the position of the thrusters about O as shown in Figure 2. $\boldsymbol{T_a}$ for the combined system can be written as shown in equation (1. 6), where, Column 1 and 6 represent the effect of the transverse thrusters, column 2 & 3 and 7 & 8 of the vertical thrusters and column 4 & 5 and 9 & 10 of the axial thrusters respectively.

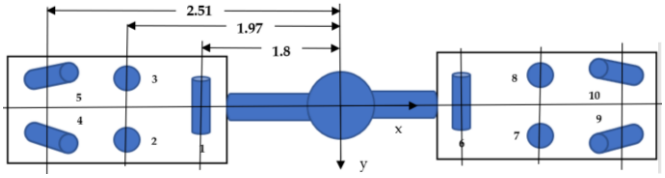

Figure 2: Allocation of the thrusters in the combined system

$$
\boldsymbol{T_a} = \begin{bmatrix}
0 & 0 & 0 & \cos(\theta) & \cos(\theta) & 0 & 0 & 0 & -\cos(\theta) & -\cos(\theta) \\
1 & 0 & 0 & \sin(\theta) & -\sin(\theta) & 1 & 0 & 0 & \sin(\theta) & -\sin(\theta) \\
0 & 1 & 1 & 0 & 0 & 0 & 1 & 1 & 0 & 0 \\
0 & l_{y2} & -l_{y3} & 0 & 0 & 0 & l_{y7} & -l_{y8} & 0 & 0 \\
0 & l_{x2} & l_{x3} & 0 & 0 & 0 & -l_{x7} & -l_{x8} & 0 & 0 \\
-l_{x1} & 0 & 0 & -l_{x4}sin(\theta) - l_{y4}\cos(\theta) & l_{x5}sin(\theta) + l_{y5}\cos(\theta) & l_{x6} & 0 & 0 & l_{x9}sin(\theta) + l_{y9}\cos(\theta) & -l_{x10}sin(\theta) - l_{y10}\cos(\theta)
\end{bmatrix}. \qquad (1.\ 6)
$$

The thrust force of a thruster can be calculated by the following equation [21]

$$f = K_T \rho D^4 |n| n. \quad (1.7)$$

Where K_T is the thrust coefficient, D is the diameter of the thruster and n is the revolution per second (rps). K_T can be found from the open water test which gives a relationship between the thrust coefficient K_T and the advance ratio of the thruster J_a. The advance ratio can be calculated as [21]

$$J_a = \frac{V_a}{nD}. \quad (1.8)$$

V_a is the velocity of the thruster through water known as advance velocity.

4. CENTRALIZED CONTROL SYSTEM DESIGN

The centralized control system is designed to get the desired motion response as well as keeping the system intact as shown in Figure 4.

- The PID controllers are applied on the error ($\boldsymbol{e}$) which is the difference between the desired ($\boldsymbol{\eta_d}$) and actual states ($\boldsymbol{\eta}$) of the combined system. PID controllers are applied on surge, sway, heave and yaw. The HAUV is statically highly stable, therefore, pitch and roll can easily restore themselves. The parameters of the PID controllers are selected considering stability, tracking and robustness. Due to nonlinear coupled dynamic model, the PID parameters at which the best motion response was achieved are of high values.
- The outcome of the controllers is given to the thrust vector ($\boldsymbol{\tau_e}$) which is multiplied by the inverse of transformation matrix ($\boldsymbol{J^{-1}}$) to get the desired thrust vector about O ($\boldsymbol{\tau_d}$).
- $\boldsymbol{\tau_d}$ is multiplied by the inverse of thrust allocation matrix ($\boldsymbol{T_a{}^{-1}}$) to achieve the desired thrust force vector ($\boldsymbol{f_d}$) for the combined system.
- The saturation limits are applied on $\boldsymbol{f_d}$ to achieve the actual thrust force vector ($\boldsymbol{f}$).
- $\boldsymbol{f}$ is given to the propulsion model of the combined system to get the actual thrust vector ($\boldsymbol{\tau}$).
- $\boldsymbol{\tau}$ is then given to the dynamic model to get the actual state vector ($\boldsymbol{\eta}$) of the combined system which is then compared with the desired state vector ($\boldsymbol{\eta_d}$) to get the error ($\boldsymbol{e}$).
- Meanwhile, the actual thrust force vectors ($\boldsymbol{f_1}$ & $\boldsymbol{f_2}$) of the individual HAUVs are given to their respective propulsion models to get the actual thrust vectors ($\boldsymbol{\tau_1}$ & $\boldsymbol{\tau_2}$). $\boldsymbol{\tau_1}$ and $\boldsymbol{\tau_2}$ are then given to the individual dynamic models to get the state vectors ($\boldsymbol{\eta_1}$ & $\boldsymbol{\eta_2}$) of the two HAUVs with respect to the combined system.
- The process continues until the desired state of the combined system is achieved.

The state vector consists of pose and velocity components. The centralized control strategy controls the states of the individual HAUVs in accordance with the states of the combined system. shows the motion response of the combined system and of the individual HAUVs in the combined system when the control system is applied to achieve the desired axial distance of 10m.

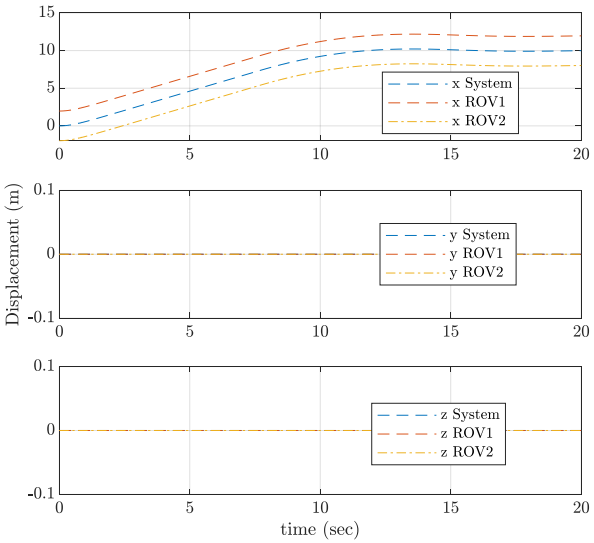

Figure 4: Motion response with a centralized control system

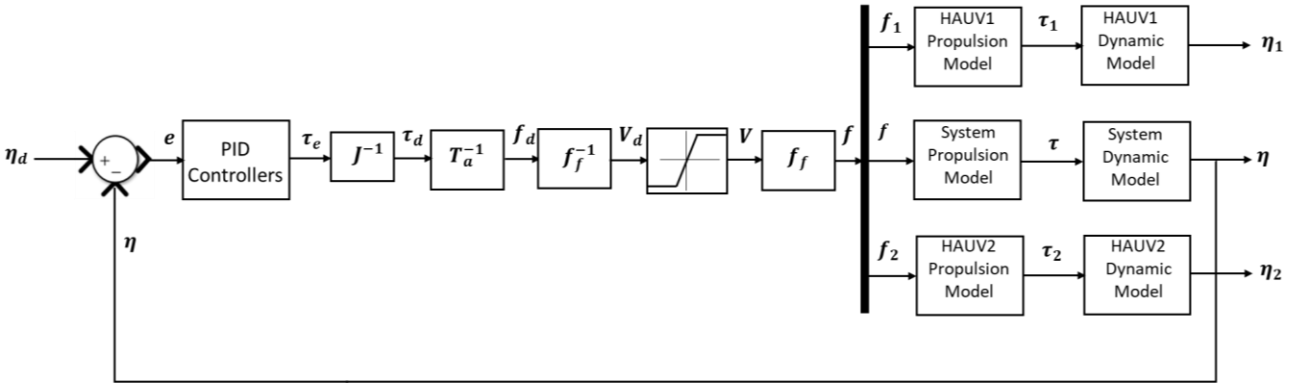

Figure 3: Centralized Control System

Note: In practice, the thrust force is a function of voltage of the thruster motor. The desired voltage vector ($\boldsymbol{V_d}$) is obtained by multiplying the desired thrust force vector ($\boldsymbol{f_d}$) by the inverse of thrust force function vector ($\boldsymbol{f_f}$). Saturation limits are applied on the voltage to achieve the actual voltage vector ($\boldsymbol{V}$). This is then multiplied by $\boldsymbol{f_f}$ to get the actual thrust force vector ($\boldsymbol{f}$), which is then given to the propulsion model to achieve the actual thrust vector ($\boldsymbol{\tau}$).

5. TRAJECTORY GENERATION AND CONTROL IMPLEMENTATION

In the above analysis, the control system is only given the target location which means, no control over the path followed by the system. This is not a recommended approach as there could be obstacles on the path followed. Therefore, a safe trajectory is generated for the system and control system is designed to follow the trajectory.

A minimum snap trajectory is generated in which the path is divided into segments. The duration of each segment is kept 10 seconds. The time step is taken to be 0.01 (which is equal to the time step of the motion simulation). Therefore, each segment has 1000 waypoints. The path between the two waypoints in a segment is represented by a 7th order polynomial which is written as [9]

$$p_i(t) = \alpha_{i0} + \alpha_{i1}\frac{t - S_{i-1}}{T_i} + \alpha_{i2}\left(\frac{t - S_{i-1}}{T_i}\right)^2 + \alpha_{i3}\left(\frac{t - S_{i-1}}{T_i}\right)^3 + \cdots + \alpha_{i7}\left(\frac{t - S_{i-1}}{T_i}\right)^7. \quad (1.\ 9)$$

$p_i(t)$ is the polynomial between two waypoints. There are in total 1000 waypoints in a segment. Therefore, there will be 999 polynomials in a segment i.e. $i = 1, \ldots \ldots, 999$.

T_i is the time step between the two waypoints i.e. 0.01 sec. on the other hand, S_i is given as

$$\text{Let } S_o = 0,\ S_i = \sum_{k=1}^{i} T_k. \quad \text{Where } i = 1, \ldots \ldots, 999. \quad (1.\ 10)$$

To solve polynomial (1. 9) for all the waypoints in the segment, first the coefficients α_{i0} needs to be solved. Where $i = 1, \ldots \ldots, 999$. and $j = 0, \ldots 7$. This makes 7992 such coefficients. To solve this, 7992 constraints are required.

1998 constraints are obtained as the polynomials pass through the waypoints i.e. [9]

$$p_i(S_{i-1}) = \omega_{i-1}. \quad i = 1, \ldots, 999. \qquad p_i(S_i) = \omega_i. \quad i = 1, \ldots, 999. \quad (1.\ 11)$$

02 constraints are obtained as the system of underwater vehicles starts and stops at rest, given as

$$\dot{p_1}(S_0) = \dot{p_n}(S_n) = 0. \quad (1.\ 12)$$

998 constraints are obtained because velocities and accelerations are continuous between the adjacent polynomial paths i.e.

$$\dot{p_i}(S_i) = \dot{p}_{i+1}(S_i). \quad i = 1, \ldots, 998. \quad (1.\ 13)$$

Further constraints are obtained due to the continuity in the higher derivatives of the trajectory and zero values at the start and end points for the higher derivatives. To compute this, the 3rd through 6th order derivatives are specified to be continuous which gives 3992 constraints, given as

$$p_i{}^k(S_i) = {p_{i+1}}^k(S_i). \quad i = 1, \ldots, 998 \text{ and } k = 3, \ldots, 6. \quad (1.\ 14)$$

Remaining 04 constraints are obtained by specifying acceleration and jerk to be zero at the start and end points, given as

$$p_1{}^k(S_0) = {p_n}^k(S_n) = 0. \quad k = 2,3. \quad (1.\ 15)$$

By this, an equal number of constraints are obtained for the number of unknown coefficients. Now write them down in the matrix form as

$$A\alpha = b. \quad (1.\ 16)$$

α is the vector containing the unknown coefficients, whereas, A and b are the matrices for all the constraints. The unknown coefficients can then be achieved by

$$\alpha = A^{-1}b. \quad (1.\ 17)$$

The centralized control system is designed with the PID controller to follow the trajectory as shown in Figure 5. The whole path is divided into three segments. The first segment takes the system to the desired depth of 2m, the second to the axial distance of 4m and the third segment brings it back to the zero depth.

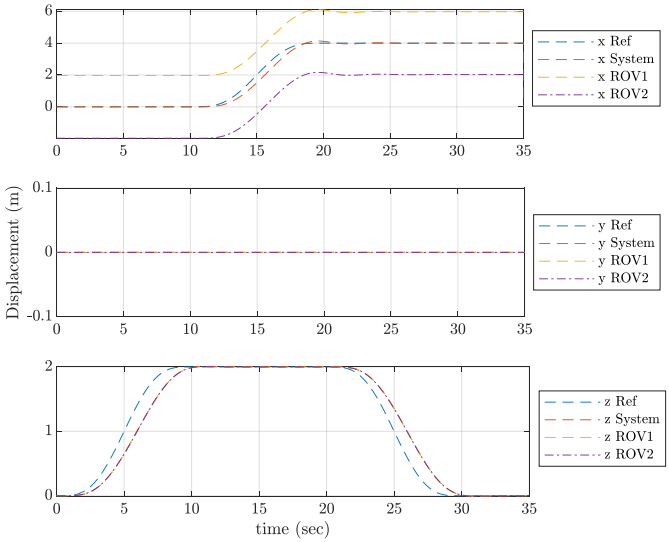

Figure 5: Motion response with a centralized control system following a trajectory

6. DISCUSSION

The technical requirements from the centralized control system design for the multi-vehicular underwater transportation are 1) the connection between the HAUVs and payload must remain intact during transportation which ensures the stability of system and the success of mission. This cannot be compromised due to the rigid connection. 2) the tracking accuracy must be ensured. This means that the whole system must follow the trajectory generated for it. However, this can be compromised by ±5%. 3) the control system should be robust enough to ensure the rigid connection and tracking accuracy even in the presence of hydrodynamic uncertainties and other disturbances.

PID controllers are used to control motion response in 6DOF. PID controller has the capability to overcome uncertainties and disturbances and ensures that the system is following the desired trajectory. The proportional regulator applies a constant gain on the error between the desired and actual

states. This reduces the error; however, tracking accuracy cannot be achieved if there are uncertainties and disturbances. Therefore, the integral regulator is applied on the accumulated tracking error and corrects it. Moreover, the higher proportional and integral gains result in oscillations. Therefore, the differential regulator is applied which anticipates the effect and applies correction.

From Figure 5, it is found that the system stably achieves the desired axial distance in 15secs while keeping the HAUVs intact to the payload during transportation. This also ensures that the uncertainties in the calculation of hydrodynamic parameters are countered for. However, the system can follow any path to achieve the desired response and can even strike an obstacle on the way. Therefore, a trajectory is generated as mentioned in Section 5 and the centralized control system is applied to follow the trajectory. It can be seen in Figure 5 that the system follows the trajectory quite stably in both the axial and vertical directions. The HAUVs adjust themselves relative to the payload to maintain the connection. The path tracking in the axial direction is up to the mark, however, a slight delay is observed in the vertical motion. The main reason is the increased weight in the vertical direction due to the payload. Nevertheless, the motion response is still within the tracking accuracy range of ±5%.

6. CONCLUSIONS

From the above analysis, it has been verified that the centralized control system with PID controllers can undertake underwater transportation using two HAUVs rigidly attached to the payload, while meeting the technical requirements. However, in the future analysis, rigid body transportation using multiple HAUVs will be required for a practical payload such as a kit for a damaged submarine or even towing a damaged submarine to the safe waters. This will require estimating the number of HAUVs to undertake transportation considering the weight of the payload. The development of dynamic model will be complicated as it will require to include the hydrodynamic and hydrostatic parameters for the increased number of vehicles and differently shaped payload. The propulsion model will also get complex by the increased size of the thrust allocation matrix for the increased number of thrusters on the added HAUVs.

REFERENCES

[1] K. Alam, T. Ray, and S. G. Anavatti, "Design and construction of an autonomous underwater vehicle," *Neurocomputing*, vol. 142, pp. 16–29, 2014.

[2] W. H. Wang, X. Q. Chen, A. Marburg, J. G. Chase, and C. E. Hann, "Design of Low-Cost Unmanned Underwater Vehicle for Shallow Waters," *IEEE/ASME Int. Conf. Mechtronic Embed. Syst. Appl.*, pp. 204–209, 2008.

[3] O. Yildiz, R. B. B. Gokalp, and A. E. E. Yilmaz, "A review on motion control of the Underwater Vehicles," *Electr. Electron. Eng.*, p. II-337-II-341, 2009.

[4] J. Ghommam, H. Mehrjerdi, M. Saad, and F. Mnif, "Formation path following control of unicycle-type mobile robots," *Rob. Auton. Syst.*, vol. 58, no. 5, pp. 727–736, 2010.

[5] J. Kennedy, A. A. Proctor, E. Gamroth, and C. Bradley, "Development of a Highly Autonomous Underwater Vehicle for Scientific Data Collection," pp. 1–11.

[6] D. R. Blidberg, "The Development of Autonomous Underwater Vehicles (AUV); A Brief Summary," *IEEE ICRA*, vol. 6500, p. 12, 2010.

[7] R. B. Wynn *et al.*, "Autonomous Underwater Vehicles (AUVs): Their past, present and future contributions to the advancement of marine geoscience," *Mar. Geol.*, 2014.

[8] C. D. Williams, "AUV systems research at the NRC-IOT: An update," *Int. Symp. Underw. Technol.*, pp. 59–73, 2004.

[9] D. Mellinger, "Trajectory Generation and Control for Quadrotors," Mechanical Engineering and Applied Mechanics PhD Thesis, University of Pennsylvania, 2012.

[10] N. Michael, J. Fink, and V. Kumar, "Cooperative manipulation and transportation with aerial robots," *Auton. Robots*, pp. 1–14, 2010.

[11] A. Yufka and M. Ozkan, "Formation-Based Control Scheme for Cooperative Transportation by Multiple Mobile Robots," *Int. J. Adv. Robot. Syst.*, vol. 12, no. 9, 2015.

[12] T. I. Fossen, *HandBook of Marine Craft Hydrodynamics and Motion Control*, 1st Ed. Sussex: John Wiley & sons, 2011.

[13] P. S. Londhe, B. M. Patre, L. M. Waghmare, and M. Santhakumar, "Robust proportional derivative (PD)-like fuzzy control designs for diving and steering planes control of an autonomous underwater vehicle," *J. Intell. Fuzzy Syst.*, vol. 32, no. 3, pp. 2509–2522, 2017.

[14] J. Peraire and J. Widnall, "Lecture L26 - 3D Rigid Body Dynamics : The Inertia Tensor," in *Dynamics*, 2008.

[15] O. A. Eidsvik, "Identification of Hydrodynamic Parameters for Remotely Operated Vehicles," Marine Technology Master Thesis, Norwegian University of Science and Tehnology, 2015.

[16] "Moment of inertia equation ad formulas of rigid objects," *Physics about*, 2018. [Online]. Available: https://physicsabout.com/moment-of-inertia/. [Accessed: 12-Dec-2018].

[17] J. R. Morison, M. P. O'Brien, J. W. Johnson, and S. A. Schaf, "The force exerted by surface waves on piles," *Pet. Technol.*, vol. 2, no. 5, 1950.

[18] A. D. Madan and M. T. Issac, "Hydrodynamic Analysis of AUV Hulls Using Semi-empirical and CFD Approach," *Univers. J. Mech. Eng.*, vol. 5, no. 5, pp. 137–143, 2017.

[19] DNV, "Modelling and Analysis of Marine Operations," *tech. rep. DNV-RP-H103*, pp. 1–91, 2010.

[20] M. D. Mikhailov and A. P. S. Freire, "The drag coefficient of a sphere: An approximation using Shanks transform," *Powder Technol.*, vol. 237, pp. 432–435, 2013.

[21] S. Marie Mo, "Development of a Simulation Platform for ROV systems," Marine Technology Master Thesis, Norwegian University of Science and Technology, 2015.

[22] S. S. Sandøy, "System Identification and State Estimation for ROV uDrone," Marine Technology Master Thesis, Norwegian University of Science and Technology, 2016.